available at www.sciencedirect.com

ScienceDirect

journal homepage: www.elsevier.com/locate/ijrefrig

Numerical assessment of steam ejector efficiencies using CFD

Szabolcs Varga[a], *Armando C. Oliveira*[a,*], *Bogdan Diaconu*[a,b]

[a]*New Energy Technologies Unit, Faculty of Engineering, University of Porto, Rua Dr Roberto Frias, 4050-123 Porto, Portugal*
[b]*University "Constantin Brancusi" of Tg-Jiu, Str. Republicii nr. 1, 210152 Tg-Jiu, Romania*

ARTICLE INFO

Article history:
Received 28 April 2008
Received in revised form
5 January 2009
Accepted 6 January 2009
Published online 20 January 2009

Keywords:
Refrigeration system
Ejector system
Simulation
Geometry
Ejector
Computational fluid Dynamics
Calculation
Performance
Efficiency

ABSTRACT

Ejector efficiencies for the primary nozzle, suction, mixing and diffuser were determined for the first time, according to their definitions, using an axi-symmetric CFD model. Water was considered as working fluid and the operating conditions were selected in a range that would be suitable for an air-conditioner powered by solar thermal energy. Ejector performance was estimated for different nozzle throat to constant section area ratios. The results indicated the existence of an optimal ratio, depending on operating conditions. Ejector efficiencies were calculated for different operating conditions. It was found that while nozzle efficiency can be considered as constant, the efficiencies related to the suction, mixing and diffuser sections of the ejector depend on operating conditions.

Evaluation numérique de la performance d'éjecteurs avec un modèle de type dynamique numérique des fluides

Mots clés:
Système frigorifique
Système à éjecteur
Simulation
Géométrie
Éjecteur
Dynamique numérique des fluides

RÉSUMÉ

On a calculé des rendements d'éjecteurs, pour ses differents parties—lance primaire, aspiration, mélange et diffuseur—par la première fois selon les definitions théoriques, en utilisant un modèle axi-simétrique type CFD. On a considéré l'eau comme fluide de travail, et les conditions opérationelles ont été choisies de façon à être convenables à un appareil d'air conditioné alimenté par de l'énergie solaire thermique. Le comportement de l'éjecteur a été calculé pour différents ratios entre la section de la gorge et la section à diamètre constant. Les résultats indiquent qu'il y a un ratio optimum, qui dépend des conditions

* *Corresponding author.*
E-mail address: acoliv@fe.up.pt (A.C. Oliveira).
0140-7007/$ – see front matter
doi:10.1016/j.ijrefrig.2009.01.007

Calcul
Performance
Rendement

opérationelles. Les divers rendements ont été calculés pour différents conditions opérationelles. On a conclu que le rendement de la lance peut être considéré comme constant, mais les rendements d'aspiration, mélange et diffuseur dépendent des conditions opérationelles.

Nomenclature

Symbols

A	Area (m^2)
d	diameter (m)
$\mathbf{g}$	acceleration of gravity vector ($m\,s^{-2}$)
h	specific enthalpy ($J\,kg^{-1}$)
$\mathbf{I}$	identity matrix
k	thermal conductivity ($W\,m^{-1}\,K^{-1}$)
L	length (m)
$\dot{m}$	mass flow rate ($kg\,s^{-1}$)
Ma	Mach number
Q	instantaneous heat, heat load (W)
r_A	area ratio $(d_m/d_{nozz})^2$
v	average velocity ($m\,s^{-1}$)

Greek letters

γ	specific heat ratio
λ	entrainment ratio
μ	viscosity (Pa s)
ρ	density ($kg\,m^{-3}$)

Subscripts

c	condenser
Ch	chocked
d	diffuser
e	evaporator
ex	exit plane
g	generator
i,j	generic space coordinates (2D)
m	constant area section
mix	mixing
nozz	nozzle
pr	primary
s	suction
sec	secondary fluid

1. Introduction

Using low grade thermal energy instead of electricity to operate a refrigerator can have important environmental benefits, especially when it is powered by a renewable energy source (e.g. solar thermal). Ejector refrigeration is one of the most promising technologies because of its relative simplicity and low capital cost when compared to e.g. an absorption refrigerator. Furthermore, ejectors don't have moving parts, and thus require little maintenance and have a long lifespan. Even though their coefficient of performance (COP) is relatively low (0.1–0.4), with careful design they can be serious competitors to other systems. This is especially true for air-conditioning applications, which have been responsible for a large portion of the increase in electricity consumption in most developed and developing countries during the last decade.

Since the early nineties it has been realised by many researchers that it is necessary to improve the performance of ejectors in order to make them economically more attractive. Thus, a thorough understanding of their operation is essential. A number of experimental investigations have been carried out to assess the effect of ejector geometry on its performance, such as nozzle exit location (Aphornratana and Eames, 1997; Chunnanond and Aphornratana, 2004a; Eames et al., 2007), mixing chamber/nozzle area ratio (Huang and Chang, 1999; Sankarlal and Mani, 2007; Chang and Chen, 2000), tail and nozzle design (Chang and Chen, 2000; Eames, 2002), as well as the effect of working fluid (Cizungu et al., 2001; Godefroy et al., 2007; Hernandez et al., 2004; Sun, 1999). Optimal design is, however, not simple, due to the complex nature of the fluid flow mechanisms and is very sensitive to operational conditions. A deviation from design conditions can affect its performance very negatively. A review on ejector theory and applications can be found in Chunnanond and Aphornratana (2004b).

Most of the theoretical works carried out used extensions of the 1D constant pressure mixing ejector theory, first developed by Keenan et al. (1950). In this approach, a number of assumptions were made including e.g. ideal gas behaviour, negligible supply, downstream velocities etc. It was also assumed that mixing between primary (high pressure fluid coming from the generator) and secondary (low pressure fluid from evaporator) flows occurs at constant pressure starting from the point where the secondary fluid gets chocked at a certain distance from the nozzle exit. Thermodynamic irreversibilities were accounted for by introducing constant efficiencies at various points along the ejector, such as primary nozzle (η_{noz}) (Aly et al., 1999; Cizungu et al., 2005; Eames et al., 1995; El-Dessouky et al., 2002; Godefroy et al., 2007; Grazzini and Mariani, 1998; Grazzini and Rocchetti, 2002; Huang et al., 1999; Korres et al., 2002; Rogdakis and Alexis, 2000; Selvaraju and Mani, 2004; Sun, 1996; Tyagi and Murty, 1985; Yapici and Ersoy, 2005; Yu et al., 2006, 2008; Zhu et al., 2007), mixing (η_{mix}) (Aly et al., 1999; Cizungu et al., 2001; Eames et al., 1995; Godefroy et al., 2007; Huang et al., 1999; Korres et al., 2002; Rogdakis and Alexis, 2000; Tyagi and Murty, 1985; Yu et al., 2006) and diffuser efficiencies (η_{dif}) (Aly et al., 1999; Cizungu et al., 2001, 2005; Eames et al., 1995; El-Dessouky et al., 2002; Godefroy et al., 2007; Grazzini and Mariani, 1998; Grazzini and Rocchetti, 2002; Huang et al., 1999; Korres et al., 2002; Rogdakis and Alexis, 2000; Selvaraju and Mani, 2004; Sun, 1996; Tyagi and Murty, 1985; Yapici and Ersoy, 2005; Yu et al., 2006, 2008). In some of the works, the losses during the mixing process were expressed in terms of a friction coefficient (f) (Cizungu et al., 2001, 2005; Selvaraju

and Mani, 2004). These constants were in some cases selected arbitrarily (e.g. Tyagi and Murty, 1985), in others taken from literature (e.g. Aly et al., 1999; Cizungu et al., 2005) or selected such that the experimentally measured performance data would fit best to the predicted model values (e.g. Eames et al., 1995; Huang et al., 1999). Grazzini and Rocchetti (2002) used a "trial and error" approach by comparing the solution from a 1D model to computational fluid dynamics (CFD) results for a two-stage ejector. Unfortunately, the results of the CFD model were not presented. Even though these efficiencies have physical meaning, in this latter case they essentially worked as correction factors. Huang et al. (1999) state that their model based on the constant pressure mixing theory can be considered as semi-empirical because of the same reasoning. Aly et al. (1999), however, pointed out that a 20% change in the nozzle efficiency affects the entrainment ratio by 25%. Unfortunately there is no information available in the literature on what are the factors influencing these values.

CFD tools have been proved to be valuable tools for understanding and analysing complex fluid flow problems, such as the entrainment and mixing processes in ejectors. Bartosiewicz et al. (2005) compared the pressure distribution by using different turbulence models for the simulation of an ejector with experimental data. It was concluded that, for certain conditions, simulated results were in excellent agreement with measured data. However, the choice of air as a working fluid and other test conditions were not very fortunate, especially when a cooling cycle is concerned. Later they extended their work using R142b as the working fluid (Bartosiewicz et al., 2006). Rusly et al. (2005) presented CFD results compared to published experimental data and 1D model predictions, using R141b. The effect of ejector geometry on the flow field was investigated. It was pointed out that according to CFD model results, 1D model assumptions were not met under test conditions. In this work, evaporator temperatures were very high for a simple ejector cooling cycle (32 °C). Sriveerakul et al. (2007a) simulated a steam ejector under different operating conditions. It was concluded that the effective area, where the secondary fluid gets chocked, exists as assumed in the 1D model; however it is very difficult to locate. The transverse shock assumption of the 1D model was opposed by CFD, indicating a series of oblique shock waves (shock train). Sriveerakul et al. (2007b) validated CFD with experimental results using water as working fluid. A good agreement between experiment and simulation was obtained for the ejector performance indicators. However, it was found that both critical back pressure and entrainment ratio were slightly under predicted by the model. Pianthong et al. (2007) analysed the performance of a steam ejector for different operating conditions and some geometrical factors (nozzle exit position and throat length). It was demonstrated that a computationally demanding 3D model resulted in similar pressure distribution compared to a less demanding axi-symmetrical case. The results indicated that CFD under predicted the critical back pressure, just as in Sriveerakul et al. (2007b). Ejectors can also be used for other applications besides refrigeration. A CFD study on using ejectors for gas-liquid contact enhancement can be found in Kandakure et al. (2005).

The validity of the 1D model is highly dependent on the efficiency constants. No information was found in the open literature on estimating these constants, according to their definitions. Therefore, the primary objective of this work was to assess ejector efficiencies (nozzle, mixing and diffuser) with a more fundamental approach, by using an axi-symmetric CFD model and steam as a driving fluid. Primary nozzle and diffuser efficiencies were determined by comparing simulated enthalpies to an isentropic process. Mixing efficiencies were calculated according to the different definitions available in the literature.

2. Ejector operation and performance

A typical ejector is presented in Fig. 1. The high pressure motive (primary) fluid coming from the steam generator (g) leaves the primary nozzle at low pressure and high velocity. This draws the low pressure (secondary) fluid from the evaporator (e) through the suction chamber. A shear layer between the motive and secondary fluid develops and thus the secondary fluid is accelerated to sonic velocity (mixing). This condition is often referred to as double chocking. The location of the mixing section depends on operating conditions and ejector geometry, but should ideally take place somewhere in the constant area section (m) or in the beginning of the diffuser. In the diffuser the mixed fluid is then decelerated and recompressed. The exit pressure depends on the conditions in the condenser of the ejector refrigeration cycle determined by the condensing temperature.

A detailed description of the mixing process is not simple, since the motive fluid flow is characterised by a series of oblique/normal shock waves called the shock train (Bartosiewicz et al., 2006), after expanding through the primary nozzle. During this process its static pressure tends to increase until it levels with the pressure of the secondary fluid. After the mixing process is completed, the resulting flow undergoes a final shock resulting in subsonic conditions. The pressure is then further increased in the subsonic diffuser. 1D models are not capable of predicting the shock train phenomena, although it affects the performance of an ejector significantly.

Ejector performance is often measured by the entrainment ratio (λ) defined as:

$$\lambda = \frac{\dot{m}_e}{\dot{m}_g} \tag{1}$$

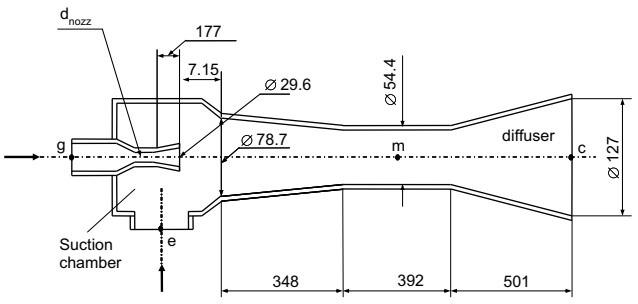

Fig. 1 – Schematic (not scaled) view of a typical ejector indicating the dimensions used for the simulation.

For a given cooling load, the required evaporator flow rate is approximately constant. The higher the entrainment ratio is, the lower the flow rate on the primary nozzle side and consequently the required generator energy input. The entrainment ratio is related to the coefficient of performance (COP) of the cooling cycle by the following expression:

$$\mathrm{COP} = \frac{Q_e}{Q_g} = \lambda \times \frac{\Delta h_e}{\Delta h_g} \tag{2}$$

For a given ejector, the entrainment ratio is affected by both operating conditions and geometry. Ejector performance decreases with increasing generator and with decreasing evaporator pressure (temperature) (Chunnanond and Aphornratana, 2004a; Sriveerakul et al., 2007a). The effect of the condenser condition on the entrainment ratio is characterised by a critical value of pressure. Below this value the entrainment ratio remains practically constant. This independence of λ on the back pressure is probably due to the chocking of the secondary fluid (Chunnanond and Aphornratana, 2004b). Beyond the critical back pressure, λ falls quickly and backflow may occur. Amongst the geometrical factors, the area ratio between the constant area section and the primary nozzle section (r_A) seems to be one of the most important. In general, ejector performance increases with increasing r_A, which however decreases the critical back pressure (Sriveerakul et al., 2007a). Another important geometrical issue is the primary nozzle exit position. Eames et al. (2007) stated that the influence of the nozzle exit position on λ can be as high as 40%. On the other hand, Rusly et al. (2005) reported that a 20% change on the nozzle exit location did not change λ significantly. Also a smaller influence was found by Pianthong et al. (2007). However it was agreed that there was a single optimum that depends on operating conditions.

3. Ejector efficiencies

As mentioned before, most theoretical works are based on the 1D constant pressure ejector theory. Detailed discussion of this method can be found in Eames et al. (1995) and Huang et al. (1999). In order to include irreversibilities associated with the primary nozzle, suction and diffuser, friction losses were introduced by applying isentropic efficiencies to the primary nozzle, suction and diffuser. However, there is some diversity in the literature on how losses in the mixing chamber are taken into account.

The enthalpy change between inlet and outlet of the primary nozzle is smaller than that of an isentropic process. Therefore, nozzle efficiency can be defined as (Rogdakis and Alexis, 2000):

$$\eta_{nozz} = \frac{h_g - h_{nozz,ex}}{h_g - h_{nozz,ex,is}} \tag{3}$$

In order to calculate the isentropic nozzle exit enthalpy in Eq. (3), the entropy at the nozzle inlet (S_g) must be known. Assuming an ideal gas, the entropy can be easily determined from the inlet pressure and temperature. If the pressure at the nozzle exit is known, the isentropic enthalpy is obtained by:

$$h_{nozz,ex,is} = f(S_g, P_{nozz,ex}) \tag{4}$$

Suction (Cizungu et al., 2001) and diffuser (Tyagi and Murty, 1985) efficiencies can be defined in a similar manner:

$$\eta_s = \frac{h_e - h_{sec,nozz,ex}}{h_e - h_{sec,nozz,ex,is}} \tag{5}$$

$$\eta_d = \frac{h_{c,is} - h_{d,in}}{h_c - h_{d,in}} \tag{6}$$

Tyagi and Murty (1985) defined entrainment efficiency in the mixing chamber as the fraction of the kinetic energy in the motive fluid transmitted to the mixture:

$$\eta_{entr} = \frac{(\dot{m}_g + \dot{m}_e)(h_c - h_{mix})}{\dot{m}_g(h_g - h_{nozz,ex})} \tag{7}$$

Eames et al. (1995) and Huang and Huang et al. (1999) defined mixing efficiency as a momentum transfer efficiency:

$$\eta_{mix} = \frac{(\dot{m}_g + \dot{m}_e)v_{mix}}{\dot{m}_g v_{nozz,exit} + \dot{m}_e v_{sec,nozz,ex}} \tag{8}$$

Aly et al. (1999) and Korres et al. (2002) defined η_{mix} similarly to Eq. (8). However, it was assumed that the velocity of the secondary fluid at the primary nozzle exit plane was approximately zero. Yu et al. (2006) considered that losses in the mixing chamber can be written as:

$$\eta_{mix} = \left[\frac{(1+\lambda)v_{mix}}{v_{nozz,exit}}\right]^2 \tag{9}$$

Cizungu et al. (2001) and Selvaraju and Mani (2004) defined mixing losses as a friction factor (f) in the form of the well known Darcy–Weisbach equation. If the velocities and pressures at the nozzle exit plane and at the mixing section are known, then f can be calculated as:

$$f_{exit} = 2\frac{d_m}{L_m}\left[\frac{v_{nozz,exit} + \lambda v_{sec,noz,ex}}{(1+\lambda)v_{mix}} + \left(p_{noz,ex} - p_m\right)\frac{A_{mix}}{(\dot{m}_g + \dot{m}_e)v_{mix}} - 1\right] \tag{10}$$

Cizungu et al. (2001) considered f_{mix} a constant value taken from the literature. Selvaraju and Mani (2004) calculated its value according to an empirical correlation for smooth walls. This approach is inherently incorrect, since most irreversible losses along the mixing process are due to the viscous shear layer between primary and secondary flow and not to wall friction. Zhu et al. (2007) defined an isentropic expansion efficiency due to frictional losses in the suction (mixing) chamber as:

$$\eta_{exp} = \left(\frac{d'_{pr,ch}}{d_{pr,ch}}\right)^2 \tag{11}$$

In Eq. (11), $d_{pr,ch}$ is the diameter of the primary flow at the cross section where the secondary fluid gets chocked and $d'_{pr,ch}$ is the value considering an ideal case:

$$d'_{pr,ch} = \left[\frac{2+(\gamma-1)Ma^2_{pr,ch}}{2+(\gamma-1)Ma^2_{nozz,ex}}\right]^{\frac{\gamma+1}{4(\gamma-1)}} \sqrt{\frac{Ma_{nozz,ex}}{Ma_{pr,ch}}} d_{nozz,ex} \quad (12)$$

In this work, the efficiencies in Eqs. (3)–(11) were estimated according to their definition, using a CFD model discussed in the next section. Input data were calculated as mass average quantities except for pressure, in which case area averaging was applied. The equations were implemented in the EES program package (F-Chart Software, Madison, USA). Physical properties of steam were evaluated as an ideal gas using the physical property functions of EES (2007). Typical efficiency values published in the relatively recent literature are summarised in Table 1.

4. CFD model

Fluid flow in the ejector is typically compressible and turbulent. In the present case, the only reasonable simplifying assumption that could be made was axi-symmetry (Pianthong et al., 2007). The functional relationship between the three major unknown variables—temperature (T), pressure (p) and velocity vector ($\mathbf{v}$)—describing compressible flow of isotropic Newtonian fluids, is given by the conservation of energy, momentum and continuity equations, in the form of a set of partial differential equations (PDEs) (White, 1991):

continuity:

$$\frac{D\rho}{Dt} + \rho \mathrm{div}\,\mathbf{v} = 0 \quad (13)$$

momentum:

$$\rho\frac{D\mathbf{v}}{Dt} = \rho\,\mathbf{g} - \nabla p + \nabla\tau_{ij} \quad (14)$$

energy:

$$\rho\frac{Dh}{Dt} = \frac{Dp}{Dt} + \mathrm{div}(k\nabla T) + \tau_{ij}\frac{\partial v_i}{\partial x_j} \quad (15)$$

In Eqs. (14) and (15) the term τ_{ij} can be written as:

$$\tau_{ij} = \mu\left(\frac{\partial v_i}{\partial x_j} + \frac{\partial v_j}{\partial x_i} - \frac{2}{3}\mathbf{I}\,\mathrm{div}\,\mathbf{v}\right) \quad (16)$$

The turbulent behaviour was treated using the Reynolds averaging principle (RANS). The realisable version of the k-ε turbulence model was chosen in this work, since it has been applied by other authors for ejector simulation (Bartosiewicz et al., 2006; Rusly et al., 2005; Sriveerakul et al., 2007b). It was reported to predict more accurately the spreading rate of jet flows and provides better performance for separation and recirculation. The actual form of the resulting transport equations for the turbulent kinetic energy (k) and the turbulent kinetic energy dissipation rate (ε) can be found in the Fluent 6.3 User's Guide (ANSYS, 2006).

In order to solve Eqs. (13)–(15), proper boundary conditions (BCs) must be applied. Pressure boundary conditions were applied on the inlets and outlet according to saturation conditions depending on the temperatures in the generator, evaporator and condenser of the ejector cooling cycle. Heat transfer through the walls was neglected (zero heat flux). In this work, a commercial package, Fluent 6.3, was used to simulate fluid flow in the ejector. In Fluent, the space domain is subdivided into a number of small control volumes called finite volumes. For each finite volume each PDE is transformed into a set of algebraic equations and then integrated using numerical techniques. The unknown quantities were calculated for each cell centre using a combination of a segregated and a coupled algorithm. For details of the finite volume method the reader is referred to Versteeg and Malalasekera (1995).

The simulated ejector was designed using a 1D model and by the recommendations of an ejector manufacturer (Venturi Jet Pumps Ltd., Stoke on Trent, UK). Its characteristic dimensions are shown in Table 2. In order to optimise the CFD model, several mesh densities were examined from the finer to the coarser. The final structured mesh consisted of 77,050 quadrangular cells.

Table 1 – Ejector efficiencies from the literature

Reference	η_{nozz}	η_s	η_{entr}	η_{mix}	f_{mix}	η_{exp}	η_d
Aly et al., 1999	0.9			0.95			0.9
Cizungu et al., 2001	0.95	0.95			0.03		0.85
Eames et al., 1995	0.85			0.95			0.85
El-Dessouky et al., 2002	1			1			1
Godefroy et al., 2007	0.8	0.95		0.935			0.8
Grazzini and Mariani, 1998	0.9			1			0.85
Huang et al., 1999	0.95	0.85		0.8–0.84			
Huang and Chang, 1999		0.85					
Rogdakis and Alexis, 2000	0.8			0.8			0.8
Selvaraju and Mani, 2004	0.95	0.95			f(Re)		0.85
Sun, 1999	0.85						0.85
Sun, 1996	0.85						0.85
Tyagi and Murty, 1985	0.9		0.8				0.9
Yapici and Ersoy, 2005	0.85						0.85
Yu et al., 2006	0.85			0.95			0.85
Yu et al., 2008	0.9			0.85			0.85
Zhu et al., 2007	0.95–0.9	0.85				0.765–0.8075	

Table 2 – Simulated ejector dimensions

	(mm)
Primary nozzle	
Exit diameter	29.6
Diverging section length	177
Exit distance from mixing chamber	7.15
Tail	
Inlet diameter:	78.7
Constant area section diameter	54.4
Diffuser exit diameter	127
Converging section length	348
Constant area section length	239
Diffuser length	501

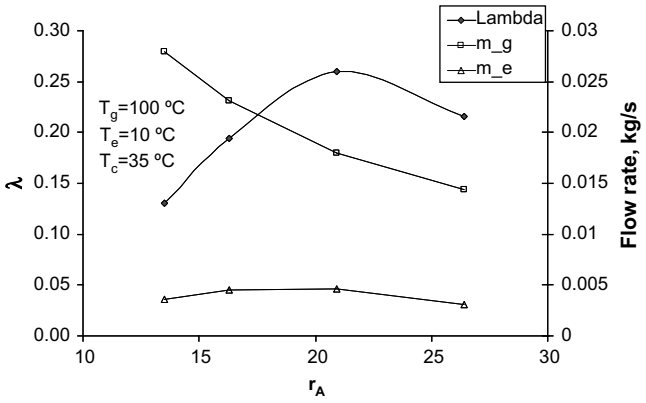

Fig. 2 – Effect of the area ratio (r_A) on entrainment ratio and mass flow rates at constant operating conditions.

5. Results and discussion

Operating conditions were considered in a range that would be suitable for an air-conditioning application using vacuum tube solar collectors for vapour generation. This would require relatively low generator temperatures. In this work, 90 °C and 100 °C were applied. Evaporator temperature was selected at a constant value of 10 °C. Condenser temperatures were varied in the range of 25–40 °C, in order to cover the entire ejector operating range. Boundary conditions at the ejector outlet were selected according to these condenser temperatures, assuming saturation conditions. The most important geometrical factors affecting ejector performance are the nozzle exit position relative to the constant area section [1] and $r_A = (d_m/d_{nozz})^2$, which is the area ratio between nozzle cross section and constant area section (Sankarlal and Mani, 2007; Ouzzane and Aidoun, 2003). In the present paper, r_A was considered in the range of 13 to 27 by changing the primary nozzle diameter while keeping d_m constant.

Fig. 2 shows entrainment ratio results as a function of r_A at constant operating conditions. A clear optimum ($\lambda = 0.26$) can be observed at an r_A value of approximately 21. This agrees well with the value of ~20 reported by Sun (1999) under similar conditions. Below the optimal area ratio the efficiency of the ejector drops rapidly. By changing r_A from 21 to 13.5, the entrainment ratio drops to 50% of the optimal value. This can be explained by over expansion of the primary flow in the mixing chamber and thus the decrease of available area for the secondary fluid. Beyond the optimal area ratio, the secondary fluid doesn't reach sonic conditions, and therefore there is a decrease in λ and eventually reverse flow can appear. A similar behaviour was observed by Rusly et al. (2005) albeit using a different working fluid (R141b) and significantly higher values of generator and evaporator temperatures. The effect of operating conditions on the optimal r_A has not been studied yet. Fig. 3 shows the entrainment ratio for different condenser conditions and area ratios, maintaining generator and evaporator temperatures. It is clear from the figure that λ increases with r_A. However, the critical back pressure (saturation at condenser temperature) decreases. For example, for a condenser temperature of 32 °C ($p_c = 4.76$ kPa), the optimal area ratio would be approximately 21 with $\lambda = 0.36$. At 35 °C, however, the same ejector would fail to operate and in this case the optimal r_A would be 16.3 with $\lambda = 0.28$.

Fig. 4 shows the calculated nozzle efficiency for 4 different nozzle diameters as a function of condenser temperature. It can be seen that ejector downstream conditions have no effect on primary nozzle efficiency. There was only a small increase in η_{nozz} with increasing nozzle diameter (0.92–0.95). Increasing the generator temperature to 100 °C did not significantly affect nozzle efficiency. Suction efficiency was also found to be constant (~0.9) when the ejector was operating below critical back pressure (see Fig. 5). However, when the exit pressure increased beyond its critical value, there was a sudden drop in its value. This is due to separation of the fluid flow from the ejector wall near the primary nozzle exit plane (see Fig. 6).

Determination of the mixing efficiency, defined in Eqs. (7)–(10), was not straightforward since the location where mixing is accomplished depends on the operating conditions. For higher back pressures, the cross section where the flow becomes subsonic moves towards the primary nozzle exit. Beyond the critical value, the secondary flow doesn't get chocked, and thus the mixing process is not completed. In this work, the mixing process was considered to be finished at the cross section where the interface velocity reached its

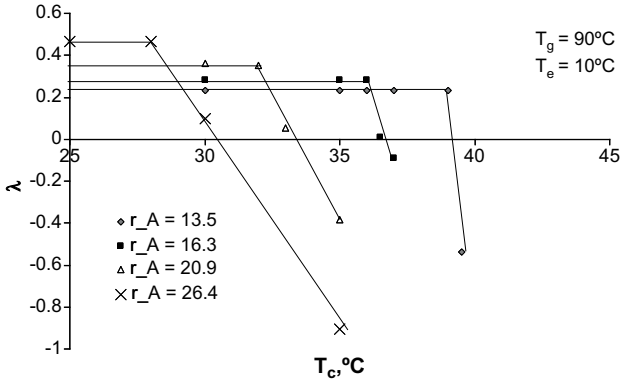

Fig. 3 – Entrainment ratio versus condenser temperature for different area ratios.

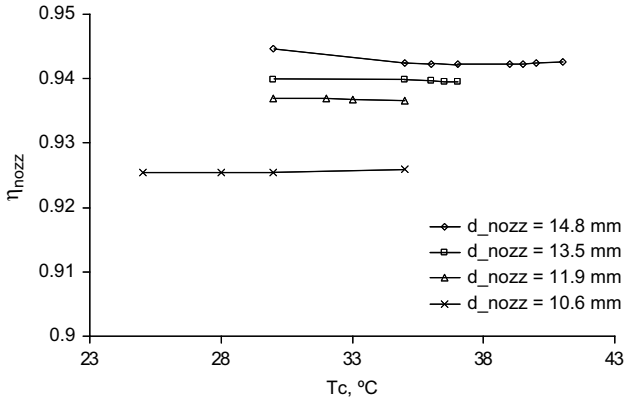

Fig. 4 – Nozzle efficiency for different nozzle diameters and condenser temperatures (T_g = 90 °C, T_e = 10 °C).

maximum before the final shock wave. When the ejector is double chocked, the mixing efficiency is not very sensitive for the selection of the mixing cross section. For example, for the ejector with $r_A = 13.5$ at $T_g = 90$ °C, $T_e = 10$ °C and back pressure corresponding to 35 °C condenser temperature, the mixing cross section was found to be 560 mm downstream from the nozzle exit (inside the constant area section). The calculated efficiency (Eq. (8)) was $\eta_{mix} = 0.90$. Selecting a cross section 90 mm upstream, resulted in an efficiency only less than 3% higher. However, beyond critical back pressure, the selection of the mixing location was very important. For example, for the ejector with $r_A = 26.4$ at $T_g = 90$ °C, $T_e = 10$ °C and back pressure corresponding to 30 °C, a similar change in the location of the mixing cross section downstream resulted in a decrease in efficiency of nearly 10% (0.82 vs. 0.75).

The results for the different irreversibilities associated to the mixing process, defined through Eqs. (7)–(10), are summarised in Table 3 for different operating conditions and area ratios. The entrainment efficiency (η_{entr}) defined by Eq. (7) varied in the range of 0.65–0.77, depending on operating conditions. These values were found to be smaller than the value reported by Tyagi and Murty (1985) (0.85). It can be seen that η_{entr} increased with condenser temperature (back pressure), which was more pronounced at higher values of the area ratio. The mixing efficiency (η_{mix}) also increased slowly with condenser temperature; however, beyond critical back

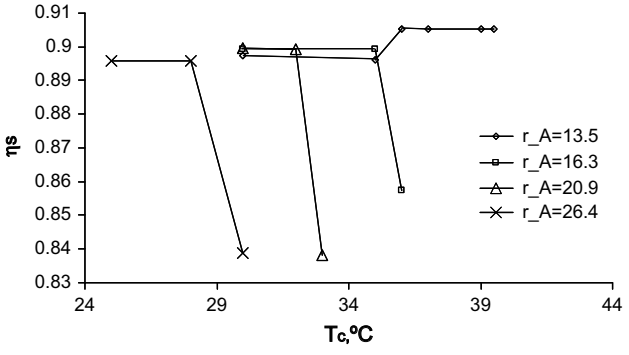

Fig. 5 – Suction efficiency as a function of condenser temperature for different area ratios.

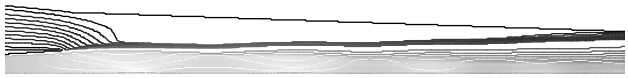

Fig. 6 – Streamlines showing flow separation near the nozzle exit plain.

pressure it dropped significantly. For example, η_{mix} defined by Eq. (8) was 0.9 for a condenser temperature of 30 °C and $r_A = 13.5$; at 39 °C, when the ejector was still working under double chocked condition, η_{mix} was 0.93, about 3% higher. For an ejector with an area ratio of 26.4, increasing back pressure beyond the critical value ($T_c = 30$ °C) resulted in a decrease of 13% in the mixing efficiency (0.92 vs. 0.82). Comparing the results at 30 °C for the different area ratios, it can be concluded that r_A had almost no effect on mixing efficiency. The friction factor (f_{mix}) defined by Eq. (10) varied in the range of 0.033–0.063, when the ejector operated in the constant entrainment ratio region. The lowest value was obtained at near critical conditions, approximately 0.033 for $r_A = 13.5$ and 0.038 for $r_A = 26.4$. These values are similar to the one used by Cizungu et al. (2001) (see Table 1). However, for lower condenser temperatures its value increased, e.g for $r_A = 16.3$ it was as high as 0.063. Beyond the critical values, f_{mix} increased considerably in all cases. The expansion efficiency defined by Eq. (11) was calculated using numerical data for the cross section where the secondary fluid interface was accelerated to Mach 1. The expansion diameter ($d_{pr,ch}$) was determined from path lines and the primary flow Mach number ($Ma_{pr,ch}$) was taken as an average. The results are shown in Table 3. It can be seen that η_{exp} varied between 0.82 and 0.94. It can be concluded that, as with the other mixing efficiencies, its value increased slowly with condenser temperature. The highest values were obtained for condenser conditions that correspond to critical conditions. However, significantly lower

Table 3 – Calculated mixing efficiencies for different operating conditions

	T_c, °C	λ	η_{entr} Eq. (7)	η_{mix} Eq. (8)	η_{mix} Aly et al. (1999)	η_{mix} Eq. (9)	f_{mix} Eq. (10)	η_{exp} Eq. (11)
$r_A = 13.5$	30	0.23	0.70	0.90	0.93	0.87	0.050	0.82
	35	0.23	0.71	0.90	0.93	0.87	0.049	0.83
	36	0.23	0.73	0.91	0.94	0.89	0.044	0.85
	37	0.23	0.73	0.92	0.95	0.89	0.042	0.89
	39	0.23	0.77	0.93	0.96	0.92	0.035	0.87
	39.5	0.23	0.77	0.93	0.96	0.93	0.033	0.87
$r_A = 16.3$	30	0.28	0.67	0.88	0.91	0.83	0.063	0.91
	35	0.28	0.70	0.90	0.93	0.87	0.051	0.90
$r_A = 20.9$	30	0.36	0.66	0.89	0.93	0.86	0.057	0.88
	32	0.35	0.72	0.90	0.94	0.89	0.050	0.87
	33	0.07	0.83	0.87	0.87	0.75	0.071	0.86
$r_A = 26.4$	25	0.46	0.65	0.90	0.95	0.91	0.051	0.93
	28	0.46	0.70	0.92	0.98	0.96	0.038	0.94
	30	0.05	0.77	0.82	0.82	0.67	0.104	0.66

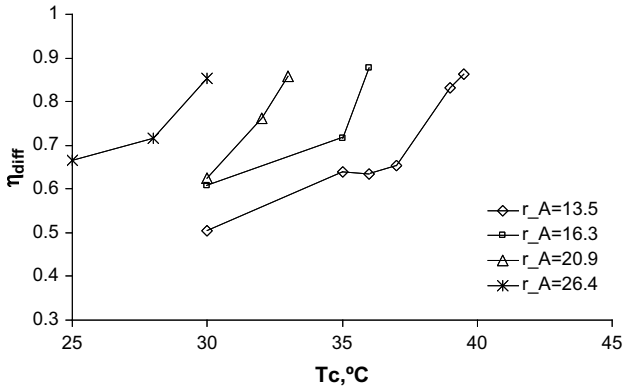

Fig. 7 – Diffuser efficiency as a function of condenser temperature for different area ratios.

efficiencies were observed for cases where the back pressure was higher than the critical value (e.g. $\eta_{exp} = 0.66$ for $r_A = 26.4$). Comparing the present results with literature data (Zhu et al., 2007) (see also Table 1), it can be stated that the calculated data were generally higher, although ejector geometry and working fluid were different.

The results for isentropic efficiency in the diffuser section are represented in Fig. 7. It is clear from the figure that η_{diff} increased considerably with condenser temperature. For example, for an area ratio of 13.5, η_{diff} was as low as 0.5 for a back pressure corresponding to a condenser temperature of 30 °C; however, at a condenser temperature of 39 °C, its value increased to 0.85. This was due to the fact that at low back pressures, the final shock wave, after which the fluid flow becomes subsonic, happened in the diffuser section, which contributed to the high losses in the diffuser. At higher back pressure, the shock wave moved back into the constant area chamber, so that the entire flow in the diffuser became subsonic and consequently losses were much smaller. It can also be seen from Fig. 7 that at a constant condenser temperature, the diffuser efficiency increases with area ratio. This can be explained by a similar reasoning. At higher r_A values (smaller primary nozzle throat diameter) the kinetic energy of the primary flow rate was smaller and consequently the final shock wave occurred further upstream, resulting in a higher diffuser efficiency. Also the mixed flow had smaller momentum, and therefore the loss through the shock wave was lower.

6. Conclusions

The performance of a simple ejector was simulated using CFD, for a range of conditions that would be suitable to operate an air-conditioning apparatus powered by solar thermal energy. The effect of the area ratio between nozzle throat and constant area chamber cross section (r_A) on entrainment ratio (λ) was studied. It was found that there is an optimal value of this geometrical factor. It was concluded that at constant evaporator and generator conditions, although λ increases with r_A, this also results in a smaller critical back pressure. Therefore, its value should be carefully selected according to operating conditions.

The different ejector efficiencies were estimated for the first time, through a most fundamental approach, using the results of a CFD model. Within the range of conditions considered in the work, the data indicated that nozzle efficiency can be considered independent of the operating conditions, and its value was only slightly affected by nozzle diameter. Suction efficiency was also constant, although its value dropped when p_c was beyond the critical value. The efficiencies defined for the mixing process (see Eqs. (7)–(11)) were more difficult to determine. It was found that in general these efficiencies increased slightly with back pressure until the critical value, beyond which they considerably dropped instead of being constant as considered in the literature. Also, in some cases the calculated values were lower than literature data, e.g. η_{entr}, and in others higher, e.g. f_{mix} and η_{exp}. It was found that the diffuser efficiency was a function of condenser conditions. An increase in back pressure, increases η_{diff}. This can be explained by the displacement of the final shock wave away from the diffuser upstream towards the primary nozzle exit.

As a final conclusion to this work, CFD analysis has proved its usefulness in analysing the complex flow behaviour in ejectors. It can provide a more fundamental approach for the assessment of ejector efficiencies and their dependence on operating and geometrical factors that are used in 1D models, which are very useful for ejector design. This work can be extended to include the effect of the working fluid, as well as other geometrical factors, on irreversibilities in the different parts of the ejector.

Acknowledgements

The authors wish to thank to Venturi Jet Pumps Ltd (UK) for their valuable contribution during the ejector design used in the present paper. The work was developed within the framework of the Mediterranean-Aircond Project, which was funded by the Commission of the European Union (DG Research), through the Energy research programme (FP6): contract INCO-CT2006-032227. The other project partners are also acknowledged.

REFERENCES

Aly, N.H., Karameldin, A., Shamloul, M.M., 1999. Modelling and simulation of steam jet ejectors. Desalination 123, 1–8.

ANSYS, 2006. Fluent 6.3 User's Guide, 2006. ANSYS Inc., Canonsburg, USA.

Aphornratana, S., Eames, I.W., 1997. A small capacity steam-ejector refrigerator: experimental investigation of a system using ejector with movable primary nozzle. Int. J. Refrig 20 (5), 352–358.

Bartosiewicz, Y., Aidoun, Z., Desevaux, P., Mercadier, Y., 2005. Numerical and experimental investigations on supersonic ejectors. Int. J. Heat Fluid Flow 26, 56–70.

Bartosiewicz, Y., Aidoun, Z., Mercadier, Y., 2006. Numerical assessment of ejector operation for refrigeration applications based on CFD. Appl. Therm. Eng 26, 604–612.

Chang, Y.-J., Chen, Y.-M., 2000. Enhancement of a steam-jet refrigerator using a novel application of the petal nozzle. Exp. Therm. Fluid Sci. 22, 203–211.
Chunnanond, K., Aphornratana, S., 2004a. An experimental investigation of a steam ejector refrigerator: the analysis of the pressure profile along the ejector. Appl. Therm. Eng 24, 311–322.
Chunnanond, K., Aphornratana, S., 2004b. Ejectors: applications in refrigeration technology. Renew. Sustain. Energy Rev. 8, 129–155.
Cizungu, K., Mani, A., Groll, M., 2001. Performance comparison of vapour jet refrigeration system with environment friendly working fluids. Appl. Therm. Eng. 21, 585–598.
Cizungu, K., Groll, M., Ling, Z.G., 2005. Modelling and optimization of two-phase ejectors for cooling systems. Appl. Therm. Eng. 25, 1979–1994.
Eames, I.W., 2002. A new prescription for the design of supersonic jet pumps: the constant rate of momentum change method. Appl. Therm. Eng 22, 121–131.
Eames, I.W., Aphornratana, S., Haider, H., 1995. A theoretical and experimental study of a small-scale steam jet refrigerator. Int. J. Refrigeration 18 (6), 378–386.
Eames, I.W., Ablwaifa, A.E., Petrenko, V., 2007. Results of an experimental study of an advanced jet-pump refrigerator operating with R245fa. Appl. Therm. Eng 27, 2833–2840.
El-Dessouky, H., Ettouney, H., Alatiqi, I., Al-Nuwaibit, G., 2002. Evaluation of steam jet ejectors. Chem. Eng. Proc. 41, 551–561.
EES, 2007. EES User Manual 2007. F-Chart Software, Madison, USA.
Godefroy, J., Boukhanouf, R., Riffat, S., 2007. Design, testing and mathematical modelling of a small-scale CHP and cooling system (small CHP-ejector trigeneration). Appl. Therm. Eng 27, 68–77.
Grazzini, G., Mariani, A., 1998. A simple program to design a multi-stage jet-pump for refrigeration cycles. Energy Conv. Manage 39, 621–633.
Grazzini, G., Rocchetti, A., 2002. Numerical optimisation of a two-stage ejector refrigeration plant. Int. J. Refrigeration 25, 621–633.
Hernandez, J.I., Dorantes, R.J., Best, R., Estrada, C.A., 2004. The behaviour of a hybrid compressor and ejector refrigeration system with refrigerants 134a and 142b. Appl. Therm. Eng 24, 1765–1783.
Huang, B.J., Chang, J.M., 1999. Empirical correlation for ejector design. Int. J. Refrigeration 22, 379–388.
Huang, B.J., Chang, J.M., Wang, C.P., Petrenko, V.A., 1999. A 1-D analysis of ejector performance. Int. J. Refrigeration 22, 354–364.
Kandakure, M.T., Gaikar, V.G., Patwardhan, A.W., 2005. Hydrodynamic aspects of ejectors. Chem. Eng. Sci. 60, 6391–6402.
Keenan, J.H., Neuman, E.P., Lustwerk, F., 1950. An investigation of ejector design by analysis and experiment. ASME J Appl. Mech 72, 299–309.
Korres, C.J., Papaioannou, A.T., Lygerou, V., Koumoutsos, N.G., 2002. Solar cooling by thermal compression The dependence of the jet thermal compressor efficiency on the compression ratio. Energy 27, 795–805.
Ouzzane, M., Aidoun, Z., 2003. Model development and numerical procedure for detailed ejector analysis and design. Appl. Therm. Eng 23, 2337–2351.
Pianthong, K., Sheehanam, W., Behnia, M., Sriveerakul, T., Aphornratana, S., 2007. Investigation and improvement of ejector refrigeration system using computational fluid dynamics technique. Energy Conv. Manage 48, 2556–2564.
Rogdakis, E.D., Alexis, G.K., 2000. Design and parametric investigation of an ejector in an air-conditioning system. Appl. Therm. Eng 20, 213–226.
Rusly, E., Aye, L., Charters, W.W.S., Ooi, A., 2005. CFD analysis of ejector in a combined ejector cooling system. Int. J. Refrigeration 28, 1092–1101.
Sankarlal, T., Mani, A., 2007. Experimental investigations on ejector refrigeration system with ammonia. Renew. Energy 32, 1403–1413.
Selvaraju, A., Mani, A., 2004. Analysis of a vapour ejector refrigeration system with environment friendly refrigerants. Int. J. Thermal Sci. 43, 915–921.
Sriveerakul, T., Aphornratana, S., Chunnanond, K., 2007a. Performance prediction of steam ejector using computational fluid dynamics: Part 2. Flow structure of a steam ejector influenced by operating pressures and geometries. Int. J. Thermal Sci. 46, 823–833.
Sriveerakul, T., Aphornratana, S., Chunnanond, K., 2007b. Performance prediction of steam ejector using computational fluid dynamics: Part 1. Validation of the CFD results. Int. J. Thermal Sci. 46, 812–822.
Sun, Da.-W., 1996. Variable geometry ejectors and their applications in ejector refrigeration systems. Energy 21 (10), 919–929.
Sun, Da.-W., 1999. Comparative study of the performance of an ejector refrigeration cycle operating with various refrigerants. Energy Conv. Manage 40, 873–884.
Tyagi, K.P., Murty, K.N., 1985. Ejector-compression systems for cooling: utilising low grade waste heat. Heat Recovery Syst 5, 545–550.
Versteeg, H.K., Malalasekera, W., 1995. An Introduction to Computational Fluid Dynamics: The Finite Volume Method. Prentice Hall, Harlow.
White, F.M., 1991. Viscous Fluid Flow, second ed. McGraw Hill, Boston.
Yapici, R., Ersoy, H.K., 2005. Performance characteristics of the ejector refrigeration system based on the constant area ejector flow model. Energy Conv. Manage 46, 3117–3135.
Yu, J., Chen, H., Ren, Y., Li, Y., 2006. A new ejector refrigeration system with an additional jet pump. Appl. Therm. Eng 26, 312–319.
Yu, J., Zhao, H., Li, Y., 2008. Application of an ejector in autocascade refrigeration cycle for the performance improvement. Int. J. Refrigeration 31 (2), 279–286.
Zhu, Y., Cai, W., Wen, C., Li, Y., 2007. Shock circle model for ejector performance evaluation. Energy Conv. Manage 48, 2533–2541.